

# Ice nanoclusters at hydrophobic metal surfaces

ANGELOS MICHAELIDES<sup>1,2\*</sup> AND KARINA MORGENSTERN<sup>3</sup>

<sup>1</sup>Fritz-Haber-Institut der Max-Planck-Gesellschaft, Faradayweg 4-6, D-14195 Berlin, Germany

<sup>2</sup>London Centre for Nanotechnology and Department of Chemistry, University College London, London WC1E 6BT, UK

<sup>3</sup>Institut für Festkörperphysik, Leibniz University of Hannover, Appelstr. 2, D-30167 Hannover, Germany

\*e-mail: [angelos.michaelides@ucl.ac.uk](mailto:angelos.michaelides@ucl.ac.uk)

Published online: 17 June 2007; doi:10.1038/nmat1940

**Studies of the structure of supported water clusters provide a means for obtaining a rigorous molecular-scale description of the initial stages of heterogeneous ice nucleation: a process of importance to fields as diverse as atmospheric chemistry, astrophysics and biology. Here, we report the observation and characterization of metal-supported water hexamers and a family of hydrated nanoclusters—heptamers, octamers and nonamers—through a combination of low-temperature scanning tunnelling microscopy experiments and first-principles electronic-structure calculations. Aside from achieving unprecedented resolution of the cyclic water hexamer—the so-called smallest piece of ice—we identify and explain a hitherto unknown competition between the ability of water molecules to simultaneously bond to a substrate and to accept hydrogen bonds. This competition also rationalizes previous structure predictions for water clusters on other substrates.**

Few physical processes are as ubiquitous or feature more prominently in our daily lives than the nucleation of water into ice. Despite having been studied since antiquity, the complexity of the intermolecular interactions between water molecules means that our molecular-scale understanding of ice nucleation remains incomplete. This is particularly true for heterogeneously catalysed nucleation in which water is prompted to nucleate through the presence of an ‘ice nucleating agent’: a microscopic seed particle of salt, sand or, in cold-adapted organisms, so-called antifreeze proteins. As most of the ice crystals encountered in our daily lives are formed with the aid of an ice nucleating agent, there is an imperative to better understand these processes and a pressing need to understand their relevance to and impact on environmental chemistry, astrophysics and biology, as well as other disciplines<sup>1–4</sup>.

The presence of the substrate on which water clustering and ice nucleation proceeds in heterogeneous nucleation brings with it challenges and opportunities. The key challenge is the added complexity that the substrate introduces: interactions between water molecules in the nascent clusters may be altered by the substrate, leading to interesting effects such as the formation of new water structures not observed in the gas phase, altered H-bond strengths or different cluster dynamics (see, for example, refs 5–8). The key opportunity the solid support brings, however, is the possibility of interrogating the properties of the adsorbed clusters with a large range of surface-sensitive probes<sup>9,10</sup>. Indeed, surface-sensitive spectroscopies (vibrational and electronic) and diffraction techniques are regularly applied to provide detailed information on the properties of water clusters and water overlayers on a wide range of solid supports. And, when the substrate is electrically conducting, such as metal surfaces are, there is the unique opportunity of direct real-space visualization of the local structure of water adlayers by means of low-temperature scanning tunnelling microscopy<sup>6</sup> (LT-STM). Indeed LT-STM of water adlayers on metals has been extremely fruitful, revealing where individual water molecules adsorb<sup>5</sup> and how they diffuse

and aggregate into water clusters such as dimers and hexamers<sup>5,11,12</sup>, as well as helping to identify the structures of novel extended one-dimensional<sup>13,14</sup> (1D) or quasi-2D<sup>15</sup> ice-like chains. However, LT-STM reports of water on metals are scarce and much remains to be learned, particularly with regard to adsorbed hexamers, which are of central importance because they are the building blocks of common ice, 1h.

Here, we report a combined LT-STM and first-principles density-functional theory (DFT) study in which the initial stages of ice nucleation on the close-packed (111) surfaces of Cu and Ag are explored. We report the observation and characterization of cyclic water hexamers and a novel family of hydrated nanoclusters—heptamers, octamers and nonamers. Aside from achieving unprecedented resolution of the cyclic hexamer—the so-called smallest piece of ice<sup>16</sup>—we identify and explain a hitherto unknown competition between the ability of water molecules to simultaneously bond to a substrate and to accept H bonds. This competition also rationalizes many previous structure predictions for water clusters on other substrates<sup>7,17–21</sup>.

Figure 1 shows typical images obtained after dosing water onto Cu(111) and Ag(111) at low temperatures (17 K). The behaviour on each surface is similar, as is the behaviour of H<sub>2</sub>O and D<sub>2</sub>O. Generally, large amorphous clusters and a number of small water particles are observed, as shown in Fig. 1a. The amorphous clusters contain tens of water molecules and do not exhibit any apparent order or recurrent similarities. The smaller water particles, however, labelled in Fig. 1b–d according to the number of molecules thought to be contained within them, appear in only four characteristic representations. At the lowest coverages (~0.05 bilayers (BL)), the water particles are exclusively observed (Fig. 1b), whereas at higher coverages (~0.5 BL), they coexist with the larger amorphous clusters (Fig. 1c,d). At all coverages examined (≤1 BL), the water particles remain as discrete nanostructures and do not agglomerate or coalesce to form extended structures such as the 1D or 2D structures observed on Cu(110) and Pd(111)

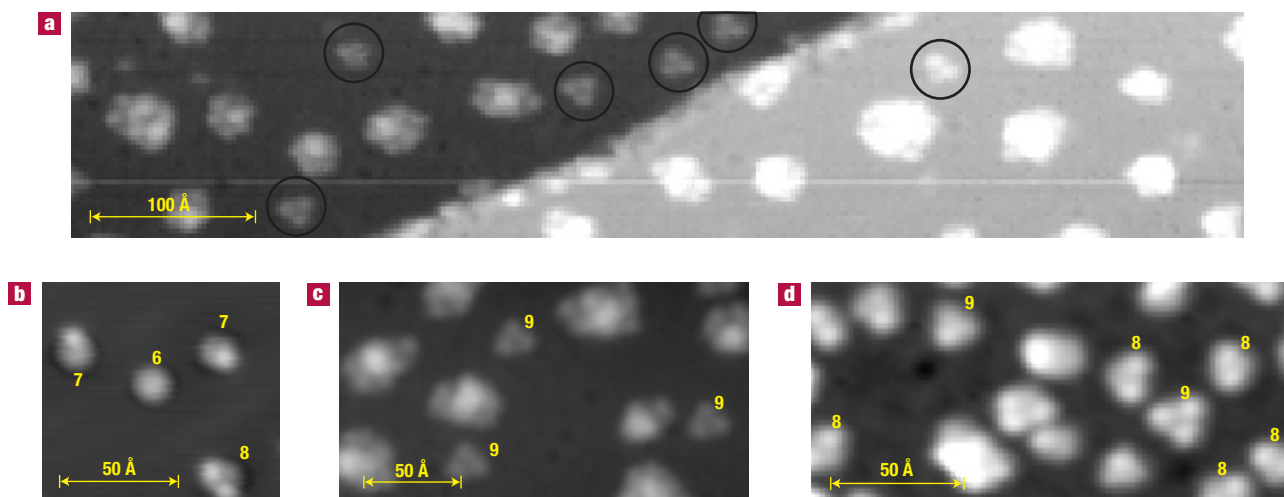


**Figure 1** Selected STM images of adsorbed water clusters on Cu and Ag. **a**, H<sub>2</sub>O on Cu(111) (120 mV and 10 pA). **b**, D<sub>2</sub>O on Ag(111) (−55 mV and 99 pA). **c**, H<sub>2</sub>O on Cu(111) (82 mV and 11 pA). **d**, H<sub>2</sub>O on Cu(111) (74 mV and 11 pA). In **a** the crystalline particles observed are circled and in **b–d** they are labelled with the number of water molecules that they comprise.

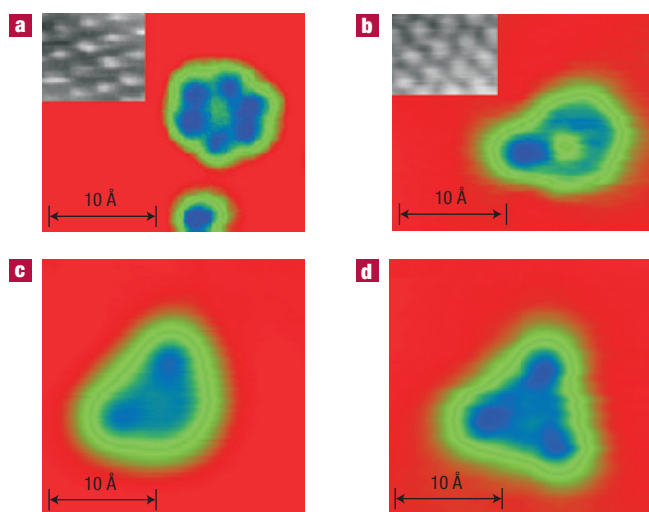


**Figure 2** High-resolution STM images of adsorbed water clusters. **a**, A H<sub>2</sub>O hexamer on Cu(111) (20 mV and 11 pA). The inset shows the Cu(111) substrate with atomic resolution (−49 mV and 29 nA). **b**, A D<sub>2</sub>O heptamer on Ag(111) (11 mV and 2 nA). The inset shows the Ag(111) substrate with atomic resolution (15 mV and 0.11 nA). **c**, A D<sub>2</sub>O octamer on Ag(111) (−21 mV and 2 nA). **d**, A D<sub>2</sub>O nonamer on Ag(111) (11 mV and 2 nA). We note that similar structures are observed with D<sub>2</sub>O and H<sub>2</sub>O on both Cu(111) and Ag(111).

or the much-discussed ice bilayer structures observed on other metal surfaces<sup>6,9,10,22–28</sup>.

High-resolution STM images such as those shown in Fig. 2 and DFT calculations lead to the conclusion that the smaller particles observed comprise 6–9 water molecules, that is, hexamers through to nonamers. From STM, a hexagon of six protrusions is observed for the smallest particle (Fig. 2a). The inset of the substrate with atomic resolution indicates that the hexagon is approximately aligned with the close-packed directions of the substrate and the

additional protrusion at the bottom of the image, an adsorbed water monomer, leads to the suggestion that the hexagonal pattern is a water hexamer. This assignment is supported by DFT, which finds that on both Cu(111) and Ag(111) the lowest energy 6H<sub>2</sub>O cluster is a cyclic hexamer with each H<sub>2</sub>O acting as a single H-bond donor and single H-bond acceptor: a so-called homodromic water cluster. This DFT structure was arrived at after testing more than 30 distinct initial configurations of the adsorbed H<sub>2</sub>O hexamer as well as several simulated annealing *ab initio* molecular dynamics simulations. In the low-energy structure identified, all H<sub>2</sub>O molecules are located close to atop sites: on Cu(111) the average displacement from the precise atop sites is 0.11 Å and on Ag(111), with the larger lattice constant, it is 0.29 Å. Interestingly, the DFT structure of the hexamer exhibits a noticeable buckling in the heights of adjacent H<sub>2</sub>O molecules (Fig. 3a, right). The vertical displacement between adjacent H<sub>2</sub>O molecules is ~0.76 Å on Cu and ~0.67 Å on Ag. Furthermore, the six nearest-neighbour O–O distances are not equal: they alternate between two characteristic values of 2.76 and 2.63 Å on Cu and 2.73 and 2.65 Å on Ag. This symmetry-breaking bond alteration is reminiscent of the alternating single and double C–C bonds in the Kekulé model of benzene (see the schematic diagram in Fig. 3a). Thus, the water hexamers identified here could be described as being ‘Kekulé-like’.

Let us turn now to the other small water particles observed (Fig. 2b–d). As the hexagonal arrangement of the moiety in Fig. 2b is still apparent but now with an additional peripheral protrusion, we conclude that this species is a water heptamer. This assignment is supported by STM measurements in which the seventh water molecule can be moved to six different positions on the hexamer by electron-induced manipulation and by DFT which finds the structure shown in Fig. 3b to be the lowest-energy structure for 7H<sub>2</sub>O molecules on Cu(111) and Ag(111). Accepting that the two smallest crystalline particles are hexamers and heptamers, it is reasonable then to assign the two remaining species (Fig. 2c,d) to water octamers and nonamers, although we note that an image of an adsorbed nonamer on Cu(111) was previously interpreted as a trimer<sup>11</sup>. The assignments of the largest observed clusters as octamers and nonamers are again supported by DFT (Fig. 3c,d). Indeed, DFT reveals that for the octamer and nonamer (as with

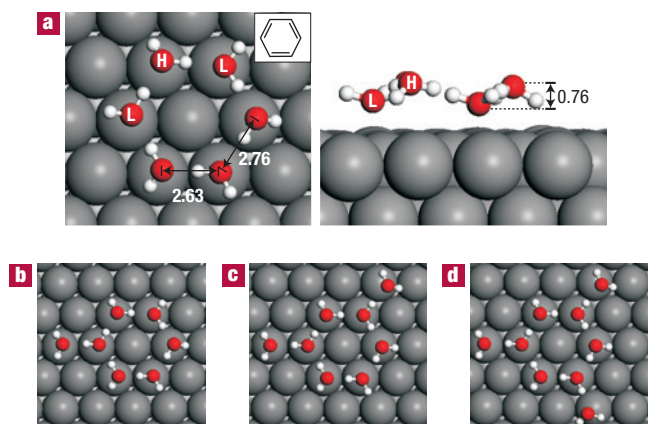


**Figure 3** Optimized structures and selected distances (Å) obtained from DFT for  $\text{H}_2\text{O}$  clusters on  $\text{Cu}(111)$ . **a**, Top and side view of the equilibrium cyclic hexamer. **b–d**, Top views of the clusters with 7–9  $\text{H}_2\text{O}$  molecules. In **a** some of the high/low  $\text{H}_2\text{O}$  molecules are labelled with an H/L. The inset in **a** shows a schematic diagram of the Kekulé structure of benzene. The low-energy structures obtained from DFT on  $\text{Ag}(111)$  are similar.

the heptamer), the additional  $\text{H}_2\text{O}$  molecules add to the low-lying  $\text{H}_2\text{O}$  molecules of the central hexagon as H-bond acceptors, that is, there is a preference for the additional  $\text{H}_2\text{O}$  molecules to bond to one of the two types of water molecule in the hexamer. It is this preference that explains the characteristic structures observed in the experiments for the octamer and nonamer with water molecules attached only to next-nearest sites of the hexamer.

The buckling of the adsorbed hexamer is important because it rationalizes the structure of the larger clusters (octamers and nonamers) that form and, as we show below, sheds new light on the nature of interfacial H bonds. However, the buckling is not observed by STM and as STM simulations within the Tersoff–Hamann approach<sup>29</sup> (not shown) indicate that the buckling in the equilibrium hexamer structure should be apparent, we must question the validity of the theoretical prediction. Therefore, we compare on  $\text{Cu}(111)$  the energy of the equilibrium buckled hexamer with an ‘ideal’ planar hexamer in which all six  $\text{H}_2\text{O}$  molecules are at the optimum height for  $\text{H}_2\text{O}$  monomer adsorption. We find that the hypothetical planar hexamer is significantly less stable than the equilibrium buckled hexamer: 122 meV per  $\text{H}_2\text{O}$ . This relative energy difference between the two structures is outside the typical absolute errors in H-bond strengths associated with the Perdew, Burke and Ernzerhof (PBE) functional used here ( $\sim 40$  meV per H bond according to refs 30 and 31). Nonetheless, it is not inconceivable that this difference is a result of our chosen computational set-up or exchange–correlation functional. Thus, we have carried out a series of tests with other DFT functionals (PBE0 (ref. 32) and the Becke three-parameter Lee, Yang, Parr hybrid functional<sup>33</sup> (B3LYP)) and with Møller–Plesset perturbation theory to second order (MP2): theoretical approaches often considered to provide more reliable energetics than the DFT-PBE set-up used here<sup>34</sup>. These tests, which were carried out on Cu clusters, are reported in Table 1 and all lead to the same conclusion: there is a considerable energetic preference ( $> 100$  meV per  $\text{H}_2\text{O}$ ) for buckling. There are several possibilities as to why the buckled structure, which is clearly favoured by first-principles theory and rationalizes the structures observed for the larger water clusters, is not apparent from the STM images. One explanation, supported by previous STM experiments for

**Table 1** Selected results of the test calculations of the energy difference,  $\Delta E$  (meV per  $\text{H}_2\text{O}$ ), between the buckled and planar cyclic  $\text{H}_2\text{O}$  hexamers on  $\text{Cu}(111)$ . A positive  $\Delta E$  indicates that the buckled hexamer is more stable than the planar one, which is always the case.

Approach	$\Delta E$ (meV per $\text{H}_2\text{O}$ )
$\text{Cu}(111)$ PBE	+122*
$\text{Cu}_{10}$ Cluster PBE	+170 <sup>†</sup> , +175 <sup>‡</sup>
$\text{Cu}_{10}$ Cluster PBE0	+170 <sup>†</sup> , +173 <sup>‡</sup>
$\text{Cu}_{10}$ Cluster B3LYP	+201 <sup>†</sup>
$\text{Cu}_{10}$ Cluster MP2	+194 <sup>†</sup> , +186 <sup>§</sup>

\* Pseudopotential plus plane-wave approach.

<sup>†</sup> All-electron with a 6-311++G(2df,pd) basis set.

<sup>‡</sup> All-electron with a 6-311++G(3df,3pd) basis set.

<sup>§</sup> All-electron with a 6-311++G(2df,pd) basis set.

$\text{H}_2\text{O}$  clusters on  $\text{Ag}(111)$  (ref. 35) and DFT calculations for  $\text{H}_2\text{O}$  on  $\text{Pd}(111)$  (ref. 36), is the influence of the electric field from the STM tip, which may reorient the molecules as they are imaged. An alternative, although not unrelated, explanation is that what is observed in experiment (Fig. 2a) may be a dynamical average of many structures sampled over the timescale of the STM measurement (seconds) rather than a single equilibrium ground-state structure. Indeed, a very short ( $\sim 3$  ps) *ab initio* molecular dynamics simulation at 100 K for the hexamer on  $\text{Cu}(111)$  supports this suggestion, revealing that its structure is highly flexible, particularly with regard to the heights of the water molecules.

So why does the buckling occur and what does it tell us about interfacial H bonds? Let us return to the hypothetical planar hexamer. In this hexamer, all six water molecules are equivalent and thus so too is their interaction with the substrate. Likewise, we would expect their interactions with each other to be the same. To examine this we define a quantity,  $\Delta\Delta\rho$  (see the caption of Fig. 4 for more details), that allows us to monitor how the electron density that lies behind our electronic-structure calculations rearranges as the interactions between adsorbed water molecules are ‘switched on’, that is,  $\Delta\Delta\rho$  is a specific type of electron density difference designed to reveal the interactions between water molecules in the adsorbed clusters. A plot of  $\Delta\Delta\rho$  is shown in Fig. 4a. As anticipated, it shows that the  $\text{H}_2\text{O}$ – $\text{H}_2\text{O}$  interactions between the adsorbed molecules in the hypothetical planar hexamer are indeed equivalent. Furthermore, the nature of the rearrangement is characteristic of that associated with H bonding: with depletion (accumulation) of density on the H (O) atoms implicated in the H bonds, similar to the H bond in ice<sup>37</sup>. We know, however, that the planar adsorbed hexamer on Cu (Ag) is  $\sim 122$  ( $\sim 76$ ) meV per  $\text{H}_2\text{O}$  less stable than the equilibrium adsorbed hexamer. This is partly a geometric effect as in this structure the water molecules do not have the optimal tetrahedral configuration for H bonding with each other. Through buckling the  $\text{H}_2\text{O}$  molecules get closer to a tetrahedral arrangement and, indeed, even in the absence of a substrate our calculations indicate that a planar cyclic hexagon gains  $\sim 50$  meV per  $\text{H}_2\text{O}$  by buckling. Within the buckled adsorption structure the two types of water molecules interact differently with the substrate, as can be seen, for example, from the density of Kohn–Sham eigenstates around each type of water molecule shown in Fig. 4c. Here, it can be seen that states located around the low-lying adsorbed molecules are lower in energy than states located around the high-lying molecules and, in particular, states of  $1b_1$  character on the low-lying molecules are shifted to lower energies through their interaction with the substrate. Ogasawara *et al.* have argued that, for a water bilayer on  $\text{Pt}(111)$ , this stabilization is related to a polarization of the

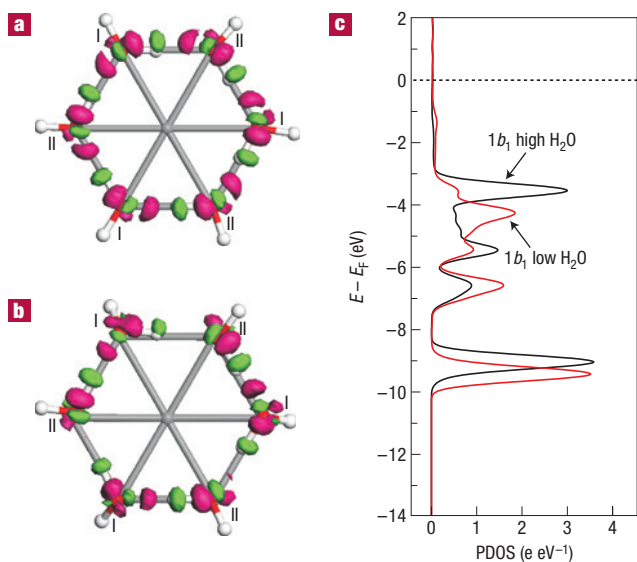


**Figure 4** Electronic structures of water hexamers on Cu(111). **a, b**, Isosurfaces of constant electron density ‘rearrangement’ ( $\Delta \Delta \rho$ ) for  $\text{H}_2\text{O}$  hexamers on Cu(111) for a hypothetical planar hexamer (**a**) and for the equilibrium (buckled) hexamer (**b**).  $\Delta \Delta \rho$  reveals  $\text{H}_2\text{O}$ – $\text{H}_2\text{O}$  bonding in the adsorbed clusters. It is defined as  $\Delta \Delta \rho = \rho_{\text{H}_2\text{O}/\text{Cu}} + \rho_{\text{Cu}} - \rho_{3\text{H}_2\text{O},\text{I}/\text{Cu}} - \rho_{3\text{H}_2\text{O},\text{II}/\text{Cu}}$ , where  $\rho_{\text{H}_2\text{O}/\text{Cu}}$  and  $\rho_{\text{Cu}}$  are the electron densities of the total adsorption systems and the isolated Cu surfaces.  $\rho_{3\text{H}_2\text{O},\text{I}/\text{Cu}}$  and  $\rho_{3\text{H}_2\text{O},\text{II}/\text{Cu}}$  are the electron densities of two subsets of the six adsorbed  $\text{H}_2\text{O}$  molecules, as labelled in **a** and **b**. Pink isosurfaces correspond to regions of electron accumulation and green isosurfaces to regions of electron depletion in units of density change equal to  $5 \times 10^{-2} \text{ e} \text{ \AA}^{-3}$ . **c**, Projected density of states (PDOS) for the equilibrium hexamer on Cu(111), projected onto the high-lying (black line) and low-lying (red line) types of water molecule. Peaks that are mostly of  $1b_1$  character (as determined from inspection of the density of the individual Kohn–Sham eigenstates) are indicated. The energy zero is the Fermi level ( $E_F$ ).

substrate’s electron density which minimizes the Pauli repulsion between the  $1b_1$  orbital and the substrate<sup>23</sup>. As the  $1b_1$  orbital of  $\text{H}_2\text{O}$  is also implicated when  $\text{H}_2\text{O}$  acts as a H-bond acceptor, the low-lying  $\text{H}_2\text{O}$  molecules are thus rendered poor H-bond acceptors through their interaction with the substrate. Essentially we see that there is a competition between the ability of a  $\text{H}_2\text{O}$  molecule to bond with the surface and its ability to act as a H-bond acceptor. It is this competition that leads to the symmetry-breaking bond alteration in the hexamer structure with, as can be seen from the electron density rearrangement plot in Fig. 4b, the longer weaker H bonds formed when the low-lying  $\text{H}_2\text{O}$  molecules act mainly as H-bond acceptors and the stronger shorter H bonds when the high-lying  $\text{H}_2\text{O}$  molecules act mainly as H-bond acceptors.

We now discuss our results in the broader context of water adsorption on solid surfaces by first comparing the hexamers identified here with the hexamers that build adsorbed water bilayers: the most commonly discussed water overlayers on metal surfaces. In adsorbed bilayers, each hexagon comprises two types of water molecule: one that lies approximately parallel to the surface and another that lies in the plane of the surface normal. The latter has one OH bond that does not participate in the H-bonded overlayer and has the option of directing this OH into the vacuum (‘H up’ model<sup>22</sup>, Fig. 5a) or at the surface (‘H down’ model<sup>23</sup>, Fig. 5b). DFT calculations have been carried out for the H-up and H-down bilayers on Cu(111) and Ag(111) as well as for idealized adsorbed hexamers cut out of such bilayers. We find that the (non-relaxed) hexamers cut out of the bilayers,

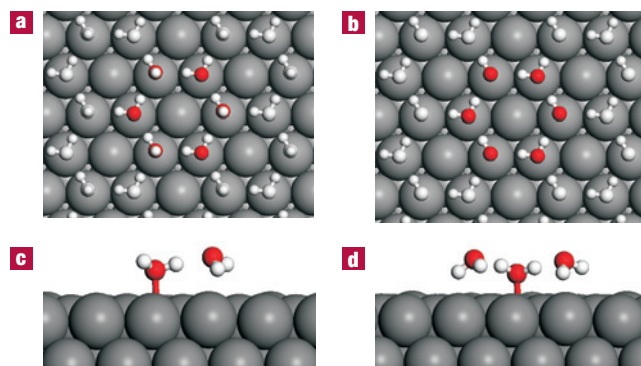


**Figure 5** Structures of model water bilayers on metal surfaces and some typical structures of small adsorbed water clusters. **a, b**, Top views of the ‘H-up’ (**a**) and ‘H-down’ (**b**) bilayer models for  $\text{H}_2\text{O}$  on hexagonal metal surfaces. A single  $\text{H}_2\text{O}$  hexagon in each type of bilayer is highlighted. **c**, Side view of the typical structure adopted for an adsorbed  $\text{H}_2\text{O}$  dimer on a metal surface. **d**, Side view of a typical structure adopted for an adsorbed  $\text{H}_2\text{O}$  trimer.

with adsorption energies of  $\sim 270$  and  $\sim 280$  meV per  $\text{H}_2\text{O}$  on Cu and Ag, respectively, are significantly less stable than the equilibrium buckled Kekulé-like hexamers identified here, which have adsorption energies of  $\sim 440$  and  $\sim 416$  meV per  $\text{H}_2\text{O}$  on Cu and Ag, respectively. Moreover, the binding energies of the equilibrium hexamers identified here are essentially identical to those in the extended 2D overlayers on each surface<sup>38</sup>. This is noteworthy because the water molecules in the discrete hexamers have fewer H bonds per molecule ( $2/\text{H}_2\text{O}$  in the isolated hexamers as opposed to  $3/\text{H}_2\text{O}$  in the bilayers), which tells us that simply counting the number of H bonds in water adlayers is not necessarily a useful way to judge their stabilities.

Next we discuss the adsorption of isolated hexamers on other metal surfaces. Specifically, we consider how the balance between  $\text{H}_2\text{O}$ – $\text{H}_2\text{O}$  and  $\text{H}_2\text{O}$ –metal bonding proceeds as we move to the surfaces of more reactive metals. To this end, DFT calculations have been carried out for cyclic hexamers adsorbed on several close-packed metal surfaces to the left of Ag in the periodic table (Pd(111), Rh(111) and Ru(0001)). It is known that as we move from right to left across the  $4d$  transition series, the interaction between water and the substrate increases<sup>9,10,39</sup>. Thus, we would expect that in the competition we have identified here between  $\text{H}_2\text{O}$ –metal bonding and the acceptance of H bonds at some stage it would no longer be favourable for hexamers to sacrifice  $\text{H}_2\text{O}$ –metal bonds so as to strengthen H bonds. We find, precisely as anticipated, that the tendency to buckle diminishes on going from Pd to Ru, but it is only on Ru that the planar structure is more favourable than the buckled one. Specifically, DFT calculations for initially flat and buckled hexamers on Pd, Rh and Ru show that after relaxation the buckled structure is favoured over the planar one by  $\sim 25$  meV per  $\text{H}_2\text{O}$  on Pd and by  $\sim 10$  meV per  $\text{H}_2\text{O}$  on Rh. On Ru, the planar hexamer structure is favoured over the buckled one by  $\sim 10$  meV per  $\text{H}_2\text{O}$ , which is consistent with a previous report of a planar hexamer on Ru (ref. 27). Thus, the buckling of the hexamers and the associated Kekulé-like alteration in the  $\text{H}_2\text{O}$ – $\text{H}_2\text{O}$  distances seems to be a rather general phenomenon of water hexamer adsorption. It is interesting to note that this periodic variation in the balance between  $\text{H}_2\text{O}$ – $\text{H}_2\text{O}$  and  $\text{H}_2\text{O}$ –metal bonding identified here is reminiscent of ion solvation in water where a competition between ion– $\text{H}_2\text{O}$  and  $\text{H}_2\text{O}$ – $\text{H}_2\text{O}$  bonding exists, with certain ions known as ‘structure makers’ and

others as ‘structure breakers’ according to the influence they have on the first hydration sphere<sup>40–42</sup>.

Finally, we briefly consider if the insight gleaned from this work can be used to rationalize the structures of adsorbed water clusters on solid surfaces in general. We do not expect that the competition identified here will be relevant to all substrates (in particular, hydrophobic graphite surfaces<sup>43,44</sup> and certain hydroxylated silicate surfaces in which the nature of the interaction of water with the substrate is distinctly different from that experienced here), however, the competition does rationalize previous structure predictions on a wide range of substrates. For example, calculations of water dimers on numerous metal (Pd (ref. 7), Pt (ref. 18) and Ni (ref. 20), and also here we have computed dimers on Cu(111) and Ag(111)) and non-metal (NaCl (refs 19,21) and BaF<sub>2</sub> (ref. 17)) surfaces all predict an asymmetric buckled structure for the dimer with the H-bond acceptor noticeably further (~0.5 Å) from the surface than the H-bond donor. The typical structure of an adsorbed H<sub>2</sub>O dimer is shown in Fig. 5c, which can now be understood by recognizing that the interaction of a water molecule with a substrate diminishes its ability to accept H bonds but not necessarily its ability to donate H bonds. Likewise, calculations for water trimers on Ni(111) (ref. 20) and trimers on Cu(111) computed as part of this study predict an asymmetric structure in which the H-bond acceptor molecules interact weakly with the substrate (Fig. 5d). Thus, the conclusion that there is a competition between the ability of water molecules to simultaneously bond to a substrate and to accept H bonds has some broad relevance beyond the water clusters and noble metals examined here and is likely to provide a useful way of thinking about the structures of water clusters on many other solid substrates.

## METHODS

The experiments reported here were carried out with custom-built ultrahigh vacuum STMs<sup>45</sup>. The Cu(111) and Ag(111) samples were cleaned by repetitive cycles of Ne<sup>+</sup> sputtering and annealing to 700 K. Water of milli-Q quality (10<sup>7</sup> Ω cm), which was further purified under vacuum by freeze–thaw cycles, was dosed onto the crystals through a leak valve while keeping the sample at 17 K. Measurements on Cu(111) and Ag(111) were carried out at 10 and 5 K, respectively.

The majority of the calculations reported here involve DFT within the plane-wave supercell approach as implemented in the CASTEP code<sup>46</sup> with ultrasoft pseudopotentials and the PBE (ref. 47) exchange–correlation functional. As large supercells, up to p(6 × 6), were used to accommodate the H<sub>2</sub>O clusters, thin three-layer Cu and Ag slabs were used. Test calculations for water clusters on slabs of up to nine layers thickness showed that on the thicker slabs adsorption energies and structures deviated by < 10 meV per H<sub>2</sub>O and < 0.1 Å, respectively. During structure optimizations, the top layer of metal atoms was free to relax. Monkhorst–Pack k-point meshes with the equivalent of at least 8 × 8 × 1 sampling within the surface Brillouin zone of a p(1 × 1) unit cell were used. The calculations on the Cu clusters (mostly ten-atom clusters with seven atoms in the top layer and three in the second) were carried out with the Gaussian03 code<sup>48</sup> with the basis sets listed in Table 1.

Received 27 December 2006; accepted 18 May 2007; published 17 June 2007.

## References

- Ball, P. *H<sub>2</sub>O: A Biography of Water* (Weidenfeld & Nicolson, London, 1999).
- Murray, B. J., Knopf, D. A. & Bertram, K. The formation of cubic ice under conditions relevant to Earth's atmosphere. *Nature* **434**, 202–205 (2005).
- Abbatt, J. P. D. *et al.* Solid ammonium sulfate aerosols as ice nuclei: A pathway for cirrus cloud formation. *Science* **313**, 1770–1773 (2006).
- Doxey, A. C., Yaish, M. Y., Griffith, M. & McConkey, B. J. Ordered surface carbons distinguish antifreeze proteins and their ice-binding regions. *Nature Biotechnol.* **24**, 852–855 (1996).
- Mitsui, T., Rose, M. K., Fomin, E., Ogletree, D. F. & Salmeron, M. Water diffusion and clustering on Pd(111). *Science* **297**, 1850–1852 (2002).
- Verdager, A., Sacha, G. M., Bluhm, H. & Salmeron, M. Molecular structure of water at interfaces: Wetting at the nanometer scale. *Chem. Rev.* **106**, 1478–1510 (2006).
- Ranea, V. A. *et al.* Water dimer diffusion on Pd(111) assisted by H-bond donor–acceptor tunneling exchange. *Phys. Rev. Lett.* **92**, 136104 (2004).
- Meng, S., Xu, L. F., Wang, E. G. & Gao, S. W. Vibrational recognition of hydrogen-bonded water networks on a metal surface. *Phys. Rev. Lett.* **91**, 059602 (2003).

- Thiel, P. A. & Madey, T. E. The interaction of water with solid-surfaces—fundamental-aspects. *Surf. Sci. Rep.* **7**, 211–385 (1987).
- Henderson, M. A. The interaction of water with solid surfaces: Fundamental aspects revisited. *Surf. Sci. Rep.* **46**, 5–308 (2002).
- Morgenstern, K. & Rieder, K. H. Formation of the cyclic ice hexamer via excitation of vibrational molecular modes by the scanning tunneling microscope. *J. Chem. Phys.* **116**, 5746–5752 (2002).
- Morgenstern, K. & Nieminen, J. Intermolecular bond length of ice on Ag(111). *Phys. Rev. Lett.* **88**, 066102 (2002).
- Morgenstern, M., Michely, T. & Comsa, G. Anisotropy in the adsorption of H<sub>2</sub>O at low coordination sites on Pt(111). *Phys. Rev. Lett.* **77**, 703 (1996).
- Yamada, T., Tamamori, S., Okuyama, H. & Aruga, T. Anisotropic water chain growth on Cu(110) observed with scanning tunneling microscopy. *Phys. Rev. Lett.* **96**, 036105 (2006).
- Cerdá, J. *et al.* Novel water overlayer growth on Pd(111) characterized with scanning tunneling microscopy and density functional theory. *Phys. Rev. Lett.* **93**, 116101 (2004).
- Nauta, K. & Miller, R. E. Formation of cyclic water hexamer in liquid helium: The smallest piece of ice. *Science* **287**, 293–295 (2000).
- Nutt, D. R. & Stone, A. J. Adsorption of water on the BaF<sub>2</sub>(111) surface. *J. Chem. Phys.* **117**, 800–807 (2002).
- Meng, S., Wang, E. G. & Gao, S. W. Water adsorption on metal surfaces: A general picture from density functional theory studies. *Phys. Rev. B* **69**, 195404 (2004).
- Park, J. M., Cho, J. H. & Kim, K. S. Atomic structure and energetics of adsorbed water on the NaCl(001) surface. *Phys. Rev. B* **69**, 233403 (2004).
- Sebastiani, D. & Delle Site, L. Adsorption of water molecules on flat and stepped nickel surfaces from first principles. *J. Chem. Theor. Comp.* **1**, 78–82 (2005).
- Yang, Y., Meng, S. & Wang, E. G. Water adsorption on a NaCl (001) surface: A density functional theory study. *Phys. Rev. B* **74**, 245409 (2006).
- Doering, D. L. & Madey, T. E. The adsorption of water on clean and oxygen-dosed Ru(001). *Surf. Sci.* **123**, 305–337 (1982).
- Ogasawara, H. *et al.* Structure and bonding of water on Pt(111). *Phys. Rev. Lett.* **89**, 276102 (2002).
- Michaelides, A. Density functional theory simulations of water–metal interfaces: Waltzing waters, a novel 2D ice phase, and more. *Appl. Phys. A* **85**, 415–425 (2006).
- Michaelides, A., Alavi, A. & King, D. A. Different surface chemistries of water on Ru(0001): From monomer adsorption to partially dissociated bilayers. *J. Am. Chem. Soc.* **125**, 2746–2755 (2003).
- Clay, C. & Hodgson, A. Water and mixed OH/water adsorption at close packed metal surfaces. *Curr. Opin. Solid State Mater. Sci.* **9**, 11–18 (2005).
- Haq, S., Clay, C., Darling, G. R. & Hodgson, A. Growth of intact water ice on Ru(0001) between 140 and 160 K: Experiment and density–functional theory calculations. *Phys. Rev. B* **73**, 115414 (2006).
- Schiros, T. *et al.* Structure of water adsorbed on the open Cu(110) surface: H-up, H-down, or both? *Chem. Phys. Lett.* **429**, 415–419 (2006).
- Tersoff, J. & Hamann, D. R. Theory of the scanning tunneling microscope. *Phys. Rev. B* **31**, 805 (1985).
- Ireta, J., Neugebauer, J. & Scheffler, M. On the accuracy of DFT for describing hydrogen bonds: Dependence on the bond directionality. *J. Phys. Chem. A* **108**, 5692–5698 (2004).
- Dahlke, E. E. & Truhlar, D. G. Improved density functionals for water. *J. Phys. Chem. B* **109**, 15677–15683 (2005).
- Adamo, C. & Barone, V. Toward reliable density functional methods without adjustable parameters: The PBE0 model. *J. Chem. Phys.* **110**, 6158–6170 (1999).
- Stephens, J., Devlin, F. J., Chabalowski, C. F. & Frisch, M. J. Ab-initio calculation of vibrational absorption and circular-dichroism spectra using density–functional force-fields. *J. Phys. Chem.* **98**, 11623–11627 (1994).
- Xantheas, S. S., Burnham, C. J. & Harrison, R. J. Development of transferable interaction models for water. II. Accurate energetics of the first few water clusters from first principles. *J. Chem. Phys.* **116**, 1493–1499 (2002).
- Morgenstern, K. & Nieminen, J. Imaging water on Ag(111): Field induced reorientation and contrast inversion. *J. Chem. Phys.* **120**, 10786–10791 (2004).
- Filhol, J.-S. & Bocquet, M.-L. Charge control of the water monolayer/Pd interface. *Chem. Phys. Lett.* **438**, 203–207 (2007).
- Nilsson, A. *et al.* The hydrogen bond in ice probed by soft x-ray spectroscopy and density functional theory. *J. Chem. Phys.* **122**, 154505 (2005).
- Michaelides, A., Alavi, A. & King, D. A. Insight into H<sub>2</sub>O-ice adsorption and dissociation on metal surfaces from first-principles simulations. *Phys. Rev. B* **69**, 113404 (2004).
- Michaelides, A., Ranea, V. A., de Andres, P. L. & King, D. A. General model for water monomer adsorption on close-packed transition and noble metal surfaces. *Phys. Rev. Lett.* **90**, 216102 (2003).
- Ayotte, P., Weddle, G. H. & Johnson, M. A. An infrared study of the competition between hydrogen-bond networking and ionic solvation: Halide-dependent distortions of the water trimer in the X-center dot(H<sub>2</sub>O)(3), (X = Cl, Br, I) systems. *J. Chem. Phys.* **110**, 7129–7132 (1999).
- Naslund, L.-A. *et al.* Direct evidence of orbital mixing between water and solvated transition-metal ions: An oxygen 1s XAS and DFT study of aqueous systems. *J. Phys. Chem. A* **107**, 6869–6876 (2003).
- Robertson, W. H., Diken, E. G., Price, E. A., Shin, J.-W. & Johnson, M. A. Spectroscopic determination of the OH- solvation shell in the OH-center dot(H<sub>2</sub>O)(n) clusters. *Science* **299**, 1367–1372 (2003).
- Cabera-Sanfeliu, P., Holloway, S., Kolasinski, K. W. & Darling, G. R. The structure of water on the (0001) surface of graphite. *Surf. Sci.* **532**, 166–172 (2003).
- Lin, C. S. *et al.* Simulation of water cluster assembly on a graphite surface. *J. Phys. Chem. B* **109**, 14183–14188 (2005).
- Mehlhorn, M., Gawronski, H., Nedelmann, L., Grujic, A. & Morgenstern, K. An instrument to investigate femtochemistry on metal surfaces in real space. *Rev. Sci. Instrum.* **78**, 033905 (2007).
- Segall, M. D. *et al.* First-principles simulation: Ideas, illustrations and the CASTEP code. *J. Phys. Condens. Matter* **14**, 2717–2744 (2002).
- Perdew, J. P., Burke, K. & Ernzerhof, M. Generalized gradient approximation made simple. *Phys. Rev. Lett.* **77**, 3865 (1996).
- Frisch, M. J. *et al.* *Gaussian 03. Revision C.02* (Gaussian, Inc., Wallingford, 2004).

## Acknowledgements

We are grateful to M. Scheffler for valuable discussions. K.M. is grateful to the Deutsche Forschungsgemeinschaft (DFG) for a Heisenberg scholarship. This work was conducted as part of a EURYI scheme. See [www.esf.org/euryi](http://www.esf.org/euryi). Correspondence and requests for materials should be addressed to A.M.

## Competing financial interests

The authors declare no competing financial interests.

Reprints and permission information is available online at <http://npg.nature.com/reprintsandpermissions/>